Chemotherapy Targets the Hair-Follicle Vascular Network but Not the Stem Cells

Yasuyuki Amoh[1,2,3], Lingna Li[1], Kensei Katsuoka[2] and Robert M. Hoffman[1,3]

Chemotherapy-induced alopecia is a major problem in clinical oncology. Doxorubicin, a widely used cancer chemotherapy drug, induces disruption of the hair cycle and subsequent alopecia. We show in this report that doxorubicin causes disruption of the hair-follicle-associated blood vessel network resulting in a greatly reduced density of these blood vessels. Dystrophic hair follicles were also observed with abnormal melanogenesis in the mice treated with doxorubicin. Visualization of the effect of doxorubicin on hair-follicle angiogenesis was made possible by the use of transgenic mice in which green fluorescent protein was driven by regulatory elements of the nestin gene (ND-GFP). In these transgenic mice, the hair-follicle stem cells and the follicle structure as well as the blood vessels associated with the hair follicles express ND-GFP. The hair-follicle stem cells did not appear to be affected by doxorubicin, which may explain why hair regrows after chemotherapy. These results suggest that inhibition of hair-follicle-associated angiogenesis by doxorubicin may be an important factor in hair-follicle dystrophy associated with chemotherapy-induced alopecia. The ND-GFP mouse model is thus useful for the study of the role of angiogenesis in the hair-follicle cycle and the effect of drugs on processes associated with chemotherapy-induced alopecia.

Journal of Investigative Dermatology (2007) **127,** 11–15. doi:10.1038/sj.jid.5700486; published online 13 July 2006

INTRODUCTION

Chemotherapy can induce anagen hair follicles to develop abnormalities that are termed hair-follicle dystrophy (Hendrix *et al.*, 2005). In some cases, chemotherapy induces the ''dystrophic anagen'' response pathway, a prolonged dystrophic anagen, followed by severely retarded follicular recovery. Severe follicular damage induces the dystrophic catagen pathway, and immediate anagen termination, followed by a dystrophic, abnormally shortened telogen and rapid follicular recovery. The C57BL/6J mouse model of cyclophosphamide-induced alopecia was used to define classification criteria for hair-follicle dystrophy including structure and pigmentation of the hair shaft, location, and volume of ectopic melanin granules, distension of the follicular canal, number of TUNEL-labeled keratinocytes in the hair bulb, and neural cell-adhesion molecule immunoreactivity (Hendrix *et al.*, 2005).

The hair-follicle stem cells appear to reside in the permanent upper portion of the hair follicle, the so-called bulge area (Cotsarelis *et al.*, 1990; Hoffman, 2000; Taylor *et al.*, 2000; Oshima *et al.*, 2001). We have recently reported (Li *et al.*, 2003; Amoh *et al.*, 2004, 2005a, b) that nestin, a marker for neural progenitor cells (Lendahl *et al.*, 1990; Zimmerman *et al.*, 1994; Yaworsky and Kappen, 1999), is also selectively expressed in cells of the hair-follicle bulge. Follicle bulge cells, labeled with nestin-driven green fluorescent protein (ND-GFP) in transgenic mice, behave as hair-follicle stem cells, differentiating to form much of the hair follicle during each hair growth cycle. We subsequently reported that many of the newly formed nestin-expressing blood vessels in the skin originate from the hair follicle, presumably the hair-follicle stem cells during the anagen phase (Amoh *et al.*, 2004). These blood vessels are labeled in transgenic mice by ND-GFP. The follicular origin of the ND-GFP-expressing vessels is most evident when transplanting ND-GFP-labeled follicles to unlabeled nude mice. After transplantation, fluorescent new blood vessels originate only from the labeled follicles. The vessels from the transplanted ND-GFP follicles responded to presumptive angiogenic signals from healing wounds. The ND-GFP-expressing blood vessels display the characteristic endothelial cell-specific markers CD31 and von Willebrand factor (Amoh *et al.*, 2004).

Using the ND-GFP mouse to image the hair-follicle stem cells and associated blood vessels, we demonstrate in this report that doxorubicin, a widely used cancer chemotherapy agent, causes inhibition of the ND-GFP-expressing vessels and dystrophy of the hair follicles. The hair-follicle stem cells appear not to be affected by doxorubicin. These studies suggest an important role of hair-follicle-associated blood vessels in maintaining normal hair-follicle structure and function and in chemotherapy-induced alopecia.

[1]*AntiCancer Inc., San Diego, California, USA;* [2]*Department of Dermatology, Kitasato University School of Medicine, Sagamihara, Japan and* [3]*Department of Surgery, University of California San Diego, San Diego, California, USA*

Correspondence: Dr Robert M. Hoffman, AntiCancer Inc., 7917 Ostrow Street, San Diego, California 92111, USA. E-mail: all@anticancer.com

Abbreviations: ND-GFP, nestin-driven green fluorescent protein; p.d., post-depilation

Received 1 March 2006; revised 10 May 2006; accepted 6 June 2006; published online 13 July 2006

RESULTS

Visualization of angiogenesis associated with hair-follicle cycling in ND-GFP-transgenic mice

Before depilation (telogen), the ND-GFP-expressing cells were located in the follicular bulge area and blood vessel network. The blood vessel network interconnected hair follicles via their bulge area (Figure 1b). At day 6 post-depilation (p.d.) (middle anagen), ND-GFP-expressing outer-root sheath cells were growing from ND-GFP-expressing cells located in the follicular bulge area. The ND-GFP-expressing nascent blood vessel network became more extensive in the lower part of the hair follicular bulge area (Figure 1c). At day 12 p.d. (late anagen), the ND-GFP-expressing cells were located in the follicular bulge area, outer-root sheath, and hair-follicle blood vessel network (Figure 1d). At day 18 p.d. (catagen), the ND-GFP-expressing cells were located in the follicular bulge area, outer-root sheath, and blood vessel network. The ND-GFP-expressing outer-root sheath cells were undergoing regression and degeneration, and the ND-GFP-expressing blood vessel network diminished (Figure 1e). Immunohistochemical staining showed that CD31 and GFP fluorescence colocalized in the ND-GFP-expressing blood vessels (Figure 2).

The ND-GFP-expressing blood vessel total length in the lower part of hair-follicle bulge was significantly longer at day 6, 12, and 18 p.d. (middle and late anagen, and catagen) than in telogen. The ND-GFP-expressing blood vessel length in the upper part of the hair-follicle bulge in anagen and catagen phase was comparable to that in telogen.

Vessel density in the upper part of follicle (mm/mm^2)	Vessel density in the lower part of follicle (mm/mm^2)
Day 0 (0.68±0.08)	Day 0 (0.48±0.05)
Day 3 (0.66±0.14)	Day 3 (0.51±0.06)
Day 6 (0.78±0.15)	Day 6 (0.83±0.11)
Day 12 (0.58±0.09)	Day 12 (1.16±0.17)
Day 18 (0.55±0.08)	Day 18 (0.69±0.07)
Day 30 (0.72±0.1)	Day 30 (0.57±0.11)

The data represent the mean values±SD.

The growth of blood vessels in the lower part of the hair-follicle bulge following/during anagen was significant compared to telogen ($P>0.001$) (Figure 3).

Doxorubicin causes inhibition of hair-follicle-associated blood vessel growth

Dystrophic hair follicles and melanin clumps in the mice treated with doxorubicin were noted in fresh tissue samples by day 7 p.d. (Figure 4a and b). Weak ND-GFP fluorescence was observed in the outer-root sheath (Figure 4c–e). By day 12, dystrophic hair follicles and melanin clumps appeared and ND-GFP fluorescence was no longer observed in the outer-root sheath. Furthermore, the number of ND-GFP-expressing blood vessels in the mice treated with doxorubicin was less than the control mice (Figure 5a and b). Similar observations were made in frozen sections. In contrast, the

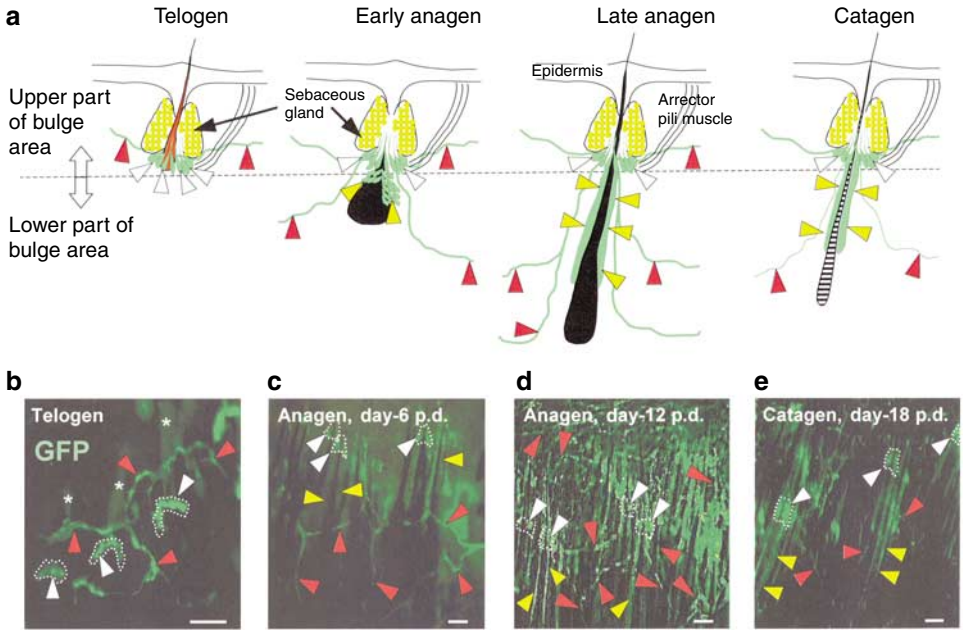

Figure 1. Time course of hair-follicle blood vessel network development during the hair cycle. (**a**) Schematic of dorsal skin hair follicles showing the location of ND-GFP-expressing cells at each stage of the hair-growth cycle. (**b–e**) The dorsal skin samples were directly observed by fluorescence microscopy with epidermis up and dermis down in ND-GFP-transgenic mice at each stage of the hair-growth cycle. White arrowheads, white dashed areas: ND-GFP-expressing hair follicular bulge area. Red arrowheads: ND-GFP-expressing blood vessels. Yellow arrowheads: ND-GFP-expressing outer-root sheath. The ND-GFP-expressing blood vessel network (red arrowheads) interconnected with the hair follicular bulge area (white arrowheads, white dashed areas). (**b**) Note: the hair shafts often displayed auto-fluorescence (asterisk). Bar = 100 μm.

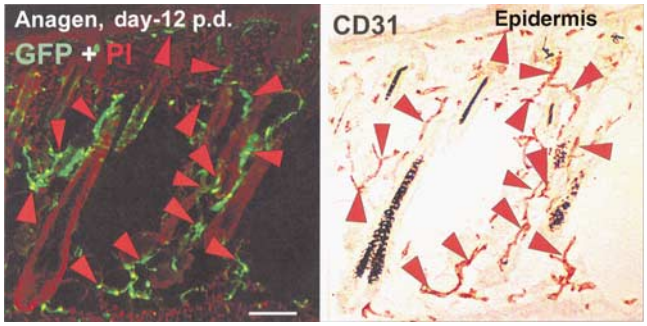

Figure 2. Immunohistochemical staining. CD31 was detected in frozen sections with the anti-rat Ig horseradish peroxidase detection kit (BD Pharmingen, San Diego, CA) following the instructions from the manufacturer. The primary antibody was CD31 mAb (1:50) (CBL1337) (Chemicon, Temecula, CA). Substrate-chromogen 3,3′-diaminobenzidine staining was used for antigen staining. The frozen sections were stained with propidium iodide (Sigma-Aldrich Inc., St Louis, MO) (5 μg/ml in phosphate-buffered saline). After this, the frozen sections were used for immunohistochemical staining. Red arrows indicated the presence of CD31, which colocalizes with ND-GFP fluorescence. Bar = 100 μm.

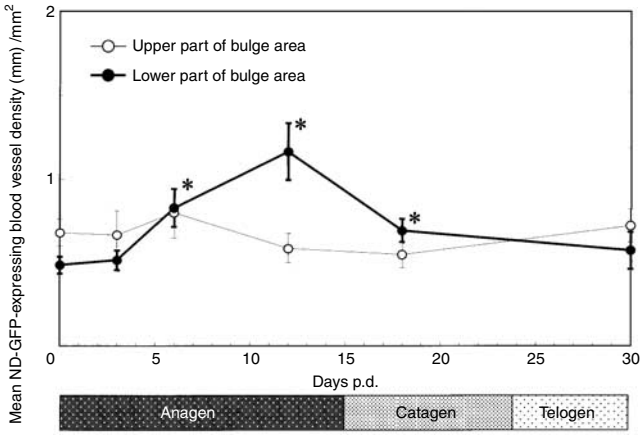

Figure 3. ND-GFP-expressing blood vessel density during the hair cycle. The skin samples were excised from dorsal skin before depilation (telogen) and at day 3 (early anagen), day 6 (middle anagen), day 12 (late anagen), day 18 (catagen), and day 30 (telogen) p.d. The frozen skin sections were used for measuring the length of ND-GFP-expressing blood vessels. At least five fields were examined for each section, derived from three differential mice per hair cycle stage. The data represent the mean values ± SD. *P < 0.001, significant compared with the results obtained before depilation (telogen).

hair follicle stem cells appeared not to be affected by doxorubicin.

The ND-GFP-expressing blood vessel total length in the lower part of hair-follicle bulge was significantly shorter in the mice treated with doxorubicin than in the control mice treated with NaCl. The ND-GFP-expressing blood vessel length in the upper part of hair-follicle bulge in the mice treated with doxorubicin was comparable to the control mice treated with NaCl. The ND-GFP-expressing blood vessel density in the upper part of the hair-follicle bulge area in doxorubicin-treated mice was 0.59 (±0.15) and in NaCl-treated mice 0.58 (±0.09). The ND-GFP-expressing blood

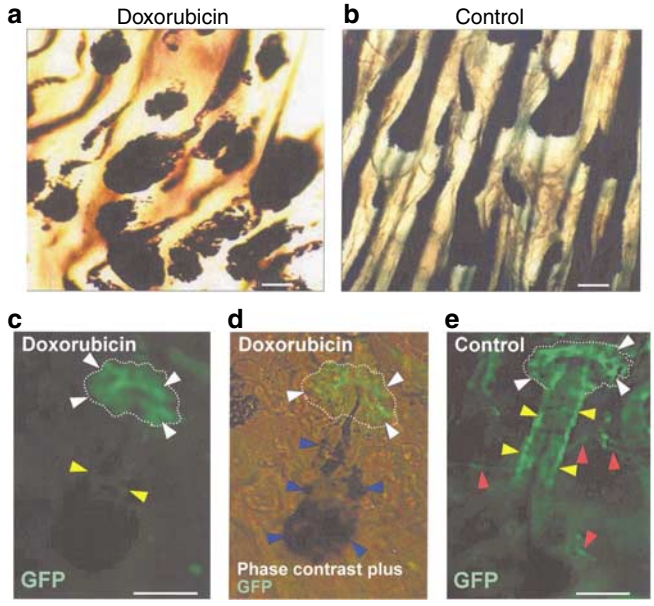

Figure 4. Effect of doxorubicin on the hair follicle and hair-follicle blood vessel network. (**a** and **b**) Dorsal skin samples were directly observed by light microscopy with epidermis up and dermis down in ND-GFP-transgenic mice. (**a**) At day 7 p.d., note the dystrophic hair follicles and the melanin clumps in the mice treated with doxorubicin. (**b**) Hair follicles in the control mice. Note the normal structure of the hair follicles. The dorsal skin samples were directly observed by fluorescence microscopy with epidermis up and dermis down in ND-GFP-transgenic mice. (**c** and **d**) At day 7 p.d., note the weak ND-GFP fluorescence in the outer-root sheath (yellow arrowheads) and the unaffected ND-GFP-expressing stem cells in the hair-follicle bulge area (white arrowheads, white dashed areas). Note the dystrophic hair follicle and the melanin clumps (blue arrowheads) in the mice treated with doxorubicin. (**e**) Normal hair follicle fluorescence, from control mice. Note the normal structure of the hair follicles, the ND-GFP-expressing stem cells in the hair-follicle bulge area (white arrowheads, white dashed areas), the ND-GFP-expressing outer-root sheath (yellow arrowheads), and ND-GFP-expressing blood vessels (red arrowheads). Bar = 100 μm.

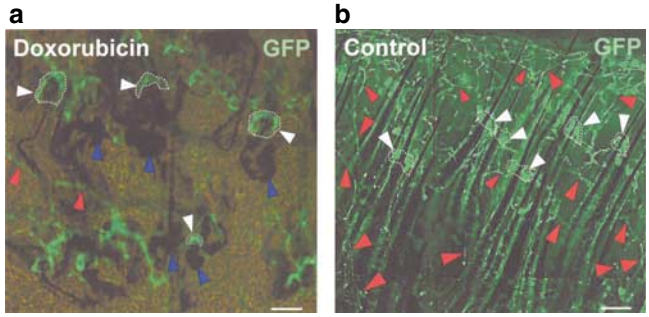

Figure 5. Dystrophic hair follicles and melanin clumping in doxorubicin-treated mice. The dorsal skin samples from ND-GFP transgenic mice were directly observed by fluorescence microscopy with epidermis up and dermis down. (**a**) At day 12 p.d., note the dystrophic hair follicles and the melanin clumps (blue arrowheads), and the lack of ND-GFP fluorescence in the outer-root sheath in the mice treated with doxorubicin. The number of ND-GFP-expressing blood vessels (red arrowheads) in the mice treated with (**a**) doxorubicin was much less than (**b**) the control mice. The hair-follicle stem cells in the bulge area were not affected by doxorubicin (white arrowheads, white dashed areas). Bar = 100 μm.

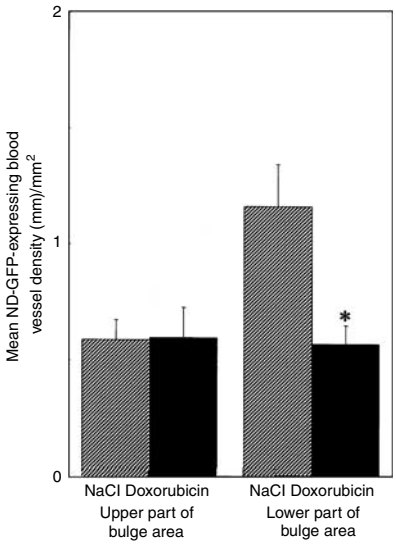

Figure 6. Effect of doxorubicin on ND-GFP-expressing blood vessel density. The ND-GFP-expressing blood vessel length in the lower part of hair-follicle bulge was significantly shorter in the mice treated with doxorubicin than in the control mice treated with NaCl. The ND-GFP-expressing blood vessel length in the upper part of hair-follicle bulge in the mice treated with doxorubicin was comparable to the control mice treated with NaCl. At least five fields were examined for each section, derived from three different mice. Treatment started 12 days p.d. The data represent the mean values + SD (*$P<0.001$). The results of inhibition of vessel length in the lower part of the follicle by doxorubicin were significant compared to the control mice treated with NaCl.

vessel density in the lower part of hair-follicle bulge area in doxorubicin-treated mice was 0.56 ($\pm$0.08) and in NaCl-treated mice 1.16 ($\pm$0.18). The data represent the mean values + SD ($P<0.001$) (Figure 6).

Frozen sections for TUNEL staining were made from the skin from mice treated with doxorubicin. We could observe apoptotic cells in sebaceous glands. However, we did not observe apoptotic cells in the ND-GFP-expressing dermal blood vessels of the mice treated with doxorubicin.

Furthermore, the ND-GFP-expressing blood vessel density in the upper part of hair-follicle bulge in the mice treated with doxorubicin was comparable to the control mice treated with NaCl (Figure 6). Most importantly, the ND-GFP-expressing blood vessel density in the lower part of hair-follicle bulge was significantly shorter in the mice treated with doxorubicin than in the control mice treated with NaCl (Figure 5). Thus, it appears that doxorubicin does not cause apoptosis in ND-GFP-expressing blood vessels but inhibits the growth of the ND-GFP-expressing blood vessels in the lower part of hair-follicle bulge.

DISCUSSION

Mecklenburg *et al.* (2000) showed that synchronized hair-follicle cycling in adolescent C57BL/6 mice is associated with substantial angiogenesis. Mecklenburg *et al.* (2000) also observed that inhibiting angiogenesis with a fumagillin derivative inhibits experimentally induced anagen development in these mice. Yano *et al.* (2001) observed perifollicular vascularization during the induced adult hair cycle and postnatal hair development. No endothelial proliferation was observed during catagen and telogen (Yano *et al.*, 2001).

Our previous observation suggests that hair-follicle stem cells can form blood vessels that form a dermal inter-follicular microvasculature network (Li *et al.*, 2003; Amoh *et al.*, 2004). In the present study, we visualized the formation of the inter-follicular microvasculature network during hair-follicle cycling using ND-GFP-expressing transgenic mice. The length of ND-GFP-expressing blood vessels increased during depilation-induced anagen development.

Doxorubicin induces disruption of the hair cycle and subsequent alopecia in the ND-GFP model. We showed that doxorubicin caused inhibition of blood vessel growth as well as inhibition of the ND-GFP-expressing outer-root sheath cells. Dystrophic hair follicles were observed in different hair cycle stages. The fact that the hair follicle stem cells were unaffected by doxorubicin may explain why hair grows back after chemotherapy.

These results suggest that doxorubicin causes inhibition of hair-follicle-associated angiogenesis and that this inhibition may play a major role in chemotherapy-induced dystrophy and alopecia. On the other hand, the hair-follicle-derived blood vessels also vascularize tumors implanted in the skin, and this process is also inhibited by doxorubicin (Amoh *et al.*, 2005a, c). This mouse model is useful for the study of the role of angiogenesis in the hair-follicle cycle as well as in tumors and the effect of chemotherapy drugs on these processes. The model can be used to determine if specific agents, selectively delivered to the hair follicle (Li and Hoffman, 1995), can accelerate the effects of chemotherapy on hair-follicle angiogenesis and associated dystrophy while still allowing tumor angiogenesis to be inhibited.

MATERIALS AND METHODS

ND-GFP-transgenic mice

Transgenic mice carrying GFP under the control of the nestin second-intron enhancer were used in this study (ND-GFP mice) (Hoffman, 2000; Mecklenburg *et al.*, 2000; Yano *et al.*, 2001; Amoh *et al.*, 2004). ND-GFP-transgenic mice were originally obtained from Dr G Enikolopov, Cold Spring Harbor Laboratory, Cold Spring Harbor, NY) (Mignone *et al.*, 2004).

Visualization of nestin expression during the hair cycle

ND-GFP mice, with almost exclusively telogen hair follicles, were anesthetized with tribromoethanol (intraperitoneal injection of 0.2 ml per 10 g of body weight of a 1.2% solution) (Amoh *et al.*, 2004). The mice were depilated with a hot mixture of rosin and beeswax to induce anagen. Skin samples were excised from the dorsal area under anesthesia before depilation (telogen) and at 48 hours, 72 hours, day-6 (middle anagen), day-12 (late anagen), day-18 (catagen) and at day-30 (telogen). The skin samples were divided into two parts, one for fluorescence microscopy and the other for frozen sections. The samples for frozen sections were embedded in tissue-freezing embedding medium and frozen at -80°C overnight. Frozen sections 10 μm thick were cut with a CM1850 cryostat (Leica, Deerfield, IL) and were air-dried.

Fluorescence microscopy

Fluorescence microscopy was carried out by using an Olympus IMT-2 inverted microscope (Melville, NY) equipped with a mercury lamp power supply (Amoh *et al.*, 2004). The microscope had a GFP filter set (Chroma Technology, Rockingham, VT).

Immunohistochemical staining

CD31 was detected in frozen sections with an anti-rat immunoglobulin horseradish peroxidase detection kit (BD Pharmingen, San Diego, CA) following instructions from the manufacturer. The primary antibody used was CD31 mAb (1:50) (CBL1337) (Chemicon, Temecula, CA). Substrate-chromogen 3,3′-diaminobenzidine staining was used for antigen staining. The frozen sections were also stained with propidium iodide (Sigma-Aldrich Inc., St Louis, MO) (5 μg/ml in phosphate-buffered saline).

Doxorubicin-induced alopecia

ND-GFP-transgenic mice, 6–8 weeks old, with almost exclusively telogen hair follicles were used (Amoh *et al.*, 2004). Mice were anesthetized with tribromoethanol for all invasive procedures. The mice were depilated by a hot mixture of rosin and beeswax. The mice were given daily intraperitoneal injections of 5 μg/g of doxorubicin or 0.9% NaCl solution at days 0, 1, and 2 p.d. Samples of dorsal skin were excised at days 7 and 12 and directly observed by light and fluorescence microscopy with epidermis up and dermis down. Skin samples for frozen sections were embedded in tissue-freezing embedding medium and frozen at -80°C overnight. Frozen sections 10 μm thick were cut with a Leica CM1850 cryostat, and were air-dried. Angiogenesis was quantified by measuring the length of ND-GFP-expressing blood vessels. All fields at $\times 40$ or $\times 100$ magnification were measured. The total length of ND-GFP-expressing nascent blood vessels was calculated. At least five fields were examined for each section, derived from three mice per hair cycle stage. Vessel density was calculated as the mean length of ND-GFP-expressing blood vessels per square millimeter. Each experimental group consisted of five mice.

TUNEL staining

Samples of dorsal skin were excised at days 6 and 12 and embedded in tissue-freezing embedding medium and frozen at -80°C overnight. Frozen sections 10 μm thick were cut with a Leica CM1850 cryostat, and air-dried. TUNEL staining was performed with the DermaTACS™ kit according to the manufacturer's instructions (R&D systems, Minneapolis, MN).

Statistical analysis

The experimental data are expressed as the mean $\pm$ SD. Statistical analysis was performed using the two-tailed Student's *t*-test.

All animal studies were conducted in accordance with the principles and procedures outlined in the NIH Guide for the Care and Use of Animals under assurance number A3873-1. Animal experiments were approved by the Institutional Animal Care and Use Committee.

CONFLICT OF INTEREST

The authors state no conflict of interest.

ACKNOWLEDGMENTS

This work was supported in part by Grant AR050933 from the National Institute of Arthritis and Musculoskeletal and Skin Disease.

REFERENCES

Amoh Y, Li L, Yang M, Jiang P, Moossa AR, Katsuoka K *et al.* (2005a) Hair follicle-derived blood vessels vascularize tumors in skin and are inhibited by doxorubicin. *Cancer Res* 65:2337–43

Amoh Y, Li L, Yang M, Moossa AR, Katsuoka K, Penman S *et al.* (2004) Nascent blood vessels in the skin arise from nestin-expressing hair-follicle cells. *Proc Natl Acad Sci USA* 101:13291–5

Amoh Y, Li L, Katsuoka K, Penman S, Hoffman RM (2005b) Multipotent nestin-positive, keratin-negative hair-follicle bulge stem cells can form neurons. *Proc Natl Acad Sci USA* 102:5530–4

Amoh Y, Yang M, Li L, Reynoso J, Bouvet M, Moossa AR *et al.* (2005c) Nestin-linked green fluorescent protein transgenic nude mouse for imaging human tumor angiogenesis. *Cancer Res* 65:5352–7

Cotsarelis G, Sun TT, Lavker RM (1990) Label-retaining cells reside in the bulge area of pilosebaceous unit: implications for follicular stem cells, hair cycle, and skin carcinogenesis. *Cell* 61:1329–37

Hendrix S, Handjiski B, Peters EM, Paus R (2005) A guide to assessing damage response pathways of the hair follicle: lessons from cyclophosphamide-induced alopecia in mice. *J Invest Dermatol* 125:42–51

Hoffman RM (2000) The hair follicle as a gene therapy target. *Nat Biotechnol* 18:20–1

Lendahl U, Zimmerman LB, McKay RD (1990) CNS stem cells express a new class of intermediate filament protein. *Cell* 60:585–95

Li L, Hoffman RM (1995) The feasibility of targeted selective gene therapy of the hair follicle. *Nat Med* 1:705–6

Li L, Mignone J, Yang M, Matic M, Penman S, Enikolopov G *et al.* (2003) Nestin expression in hair follicle sheath progenitor cells. *Proc Natl Acad Sci USA* 100:9958–61

Mecklenburg L, Tobin DJ, Muller-Rover S, Handjiski B, Wendt G, Peters EM *et al.* (2000) Active hair growth (anagen) is associated with angiogenesis. *J Invest Dermatol* 114:909–16

Mignone JL, Kukekov V, Chiang AS, Steindler D, Enikolopov G (2004) Neuron stem and progenitor cells in nestin-GFP transgenic mice. *J Comp Neurol* 469:311–24

Oshima H, Rochat A, Kedzia C, Kobayashi K, Barrandon Y (2001) Morphogenesis and renewal of hair follicles from adult multipotent stem cells. *Cell* 104:233–45

Taylor G, Lehrer MS, Jensen PJ, Sun TT, Lavker RM (2000) Involvement of follicular stem cells in forming not only the follicle but also the epidermis. *Cell* 102:451–61

Yano K, Brown LF, Detmar M (2001) Control of hair growth and follicle size by VEGF-mediated angiogenesis. *J Clin Invest* 107:409–17

Yaworsky PJ, Kappen C (1999) Heterogeneity of neural progenitor cells revealed by enhancers in the nestin gene. *Dev Biol* 205:309–21

Zimmerman L, Parr B, Lendahl U, Cunningham M, McKay R, Gavin B *et al.* (1994) Independent regulatory elements in the nestin gene direct transgene expression to neural stem cells or muscle precursors. *Neuron* 12:11–24